SIMULATION OF DECOHESION AND FRACTURE ALONG AN INTERFACE VIA GEOMETRICALLY NONLINEAR COHESIVE ELEMENTS. APPLICATION TO ADHESIVE JOINTS

Nunziante Valoroso[1], Laurent Champaney[2]

[1]Consiglio Nazionale delle Ricerche
Istituto per le Tecnologie della Costruzione
Viale Palmiro Togliatti 1473, 00155 Roma, Italy

[2]Laboratoire de Mécanique et Technologie
ENS de Cachan / CNRS UMR 8535 / Université Paris VI
61 Avenue du Président Wilson, 94235 Cachan Cedex, France

valoroso@itc.cnr.it (Nunziante Valoroso)

Abstract

This paper describes a geometrically nonlinear formulation for an interface and its application to the analysis of adhesive joints configurations failing in the fully nonlinear regime. The core of the adopted approach is that of using a cohesive-zone model to mimic the behaviour of the adhesive layer within a corotational-like element formulation, i.e. large displacements and rotations with small strains. In particular, the adherends are allowed to experience large elastoplastic deformations while the progressive interface decohesion is modelled via the damage mechanics approach developed by the authors, that is here suitably extended to include geometric effects. This gives rise to two main differences with respect to the underlying linear formulation, namely, the need for the continuous tracking of the discontinuity surface due to the explicit dependence of the cohesive tractions on the orientation of the surface itself and the presence of geometric terms in the tangent stiffness. Numerical examples and comparisons with experimental results are provided that show the ability to capture the highly nonlinear response for a single-lap joint and an asymmetric T-peel test, where fracture of the adhesive layer is accompanied by large rotations and extensive plastic deformation of the joint arms.

Keywords: Adhesive joints, Decohesion, Damage, Nonlinear kinematics, Finite elements

Presenting Author's Biography

Nunziante Valoroso. MSc in Civil Engineering, University of Naples, Italy (1996). PhD in Structural Engineering, University of Naples, Italy (2000). Research Associate, Université Paris VI, France (2000-2001). Researcher at National Research Council, Italy (2001-present). Author or co-author of more than 40 journal and conference papers. Research interests are solid mechanics, computational plasticity, unilateral and non-smooth problems, finite elements and numerical methods in engineering.

1 Introduction

Adhesive bonding is a technique of interest in a variety of industrial applications as it can offer improved performances with respect to mechanical fastening methods, basically originating from the fact that adhesive connections can transmit stresses with more uniform distributions compared to bolts and rivets. Typically, the bond region possesses a thickness that can be considered small compared to both that of the joined bodies and to its in-plane dimensions and the adhesive is likely to be the weakest link in a structural joint; hence, the adhesive layer can be conveniently schematized as a damaging interface where a cohesive process zone is lumped. The many advantages of the cohesive-zone approach over the more classical methods of Fracture Mechanics are well-known, see e.g. [1]; in particular, one of its most appealing features is that it can be easily combined with arbitrary material non-linearities of the surrounding volume.

In current implementations, cohesive interfaces are used in conjunction with zero-thickness decohesion or interface elements; these elements are located at sites where the potential crack trajectories can develop and are equipped with a nonlinear traction-relative displacement relationship describing the process zone evolution and the formation of traction-free surfaces.
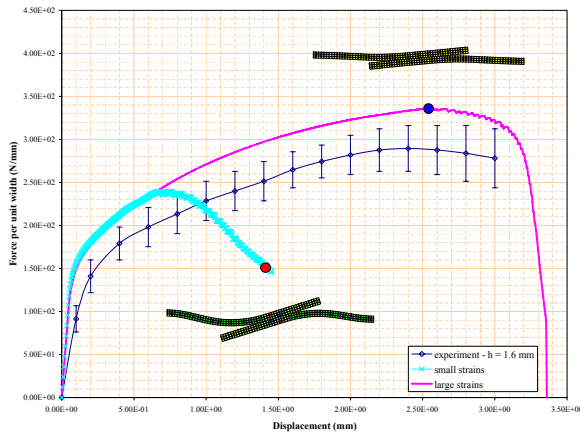
Fig. 1 Shear-lap joint. Numerical vs experimental results. Linear and nonlinear kinematics.

The present work is motivated by the authors' attempt to obtain quantitative predictions for adhesively bonded assemblies for which de-cohesion and fracture are accompanied by significant geometric effects. This is indeed a common occurrence for many joint configurations, one of the most striking examples being the single-lap shear joint for which, owing to load eccentricity, the failure mechanism can in general be captured only with the aid of a fully nonlinear analysis incorporating an appropriate fracture-based description of bond rupture (Figure 1).

To this end, the damage-mechanics-based approach developed by the authors in [2] is here suitably enhanced to account for changes in the geometry of the cohesive surface. This is done in the same spirit of a corotational-like formulation; in particular, stretching of the cohesive elements is neglected and relative displacements are taken as the only strain-producing motion for the interface. In this way the underlying "linear formulation" of the material model can be preserved under mild assumptions that also ensure frame invariance and the element implementation differ with respect to the linear one in that it is required the continuous tracking of the normal to the deformed surface, upon which the cohesive tractions explicitly depend, that also leads to geometric or initial stress terms in the tangent stiffness.

2 Nonlinear kinematics and cohesive law

The basic geometry considered is a body Ω consisting of the assembly of two adherends denoted as Ω^+ and Ω^- that are initially in contact through a planar adhesive layer S. At each instant $t \in [0, T]$ the current configuration of the structure is defined by the sets $\Omega^\pm(t) \subseteq \Re^3$ described by the displacements $\boldsymbol{u}^\pm$ from the reference configuration:

$$\boldsymbol{u}^\pm(\boldsymbol{X}, t) = \chi^\pm(\boldsymbol{X}, t) - \boldsymbol{X} \qquad (1)$$

relating the placements $\boldsymbol{X}$ in the reference configuration to the deformed ones $\boldsymbol{x}^\pm = \chi^\pm(\boldsymbol{X}, t)$ occupied at time t in the current configuration via the deformation mappings $\chi^\pm$.

In this context, the virtual power identity in the spatial description of motion reads:

$$\int_\Omega \boldsymbol{\sigma} \cdot \nabla^s(\delta\mathbf{v}) \, \mathrm{d}\Omega + \int_S \mathbf{t} \cdot [\![\delta\mathbf{v}]\!] \, \mathrm{d}S = P_{ext} \quad \forall \delta\mathbf{v} \quad (2)$$

where $\boldsymbol{\sigma}$ and $\mathbf{t}$ are the Cauchy stress and the surface traction, respectively, P_{ext} is the power of external forces, ∇^s is the symmetric gradient operator, $\delta\mathbf{v}$ the virtual spatial velocity and the symbol $[\![\cdot]\!]$ denotes the jump $(\cdot)^+ - (\cdot)^-$.

In order to formulate the problem, two main issues have to be addressed, namely, the transformation rule of the spatial velocity jump under rigid-body motions and the transformation of the area elements of the cohesive surface S. Actually, spatial fields are generally affected by a change in observer, and so is for $[\![\delta\mathbf{v}]\!]$; moreover, when contact is lost and a fracture propagates through the adhesive layer, uniqueness of the cohesive surface and its orientation are lost as well. However, both frame invariance for $[\![\delta\mathbf{v}]\!]$ and elimination of possible ambiguities in the definition of the unit normal $\mathbf{n}$ are guaranteed if one admits that before complete separation the discontinuity in displacements across the cohesive surface is small, i.e. $[\![\chi(X, t)]\!] \simeq 0$, as basic continuum mechanics arguments show [3].

In this paper we shall limit ourselves to the treatment of two-dimensional problems; the cohesive constitutive relationship used stems from the following stored energy function [2]:

$$\psi(\llbracket \boldsymbol{u} \rrbracket, \mathbf{n}, D) = \frac{1}{2} k_n^- \langle \llbracket u_n \rrbracket \rangle_-^2$$
$$+ \frac{1}{2}(1-D)\left[k_n^+ \langle \llbracket u_n \rrbracket \rangle_+^2 + k_s \llbracket u_s \rrbracket^2 \right] \qquad (3)$$

where k_n^- is a penalty stiffness that is used to prevent inter-penetration and $\langle \cdot \rangle_\pm = 1/2(\cdot \pm | \cdot |)$. In the above equation $D \in [0,1]$ is the scalar damage variable, k_n^+, k_s are undamaged interface stiffnesses, $\llbracket u_n \rrbracket = \llbracket \boldsymbol{u} \rrbracket \cdot \mathbf{n}$ and $\llbracket u_s \rrbracket = \llbracket \boldsymbol{u} \rrbracket \cdot \mathbf{s} = \llbracket \boldsymbol{u} \rrbracket - \llbracket u_n \rrbracket \mathbf{n}$ denote the normal and tangential components of the displacement jump vector across the interface, whose orientation is defined by the unit tangent vector $\mathbf{s} = \mathbf{Rn}$, where $\mathbf{R}$ denotes a proper rotation tensor such that $\mathbf{Rn} \cdot \mathbf{n} = 0$

The constitutive relationships follow from the classical thermodynamics argument; in particular, the traction vector reads:

$$\mathbf{t}(\llbracket \boldsymbol{u} \rrbracket, \mathbf{n}) = \check{\mathbf{K}} \check{\mathbf{P}}(\llbracket \boldsymbol{u} \rrbracket) + (1-D)\hat{\mathbf{K}}\hat{\mathbf{P}}(\llbracket \boldsymbol{u} \rrbracket) \qquad (4)$$

where $\check{\mathbf{P}}$ and $\hat{\mathbf{P}}$ are the complementary projectors:

$$\check{\mathbf{P}}(\llbracket \boldsymbol{u} \rrbracket) = \langle \llbracket u_n \rrbracket \rangle_- \mathbf{n}$$
$$\hat{\mathbf{P}}(\llbracket \boldsymbol{u} \rrbracket) = \langle \llbracket u_n \rrbracket \rangle_+ \mathbf{n} + \llbracket u_s \rrbracket \mathbf{Rn} \qquad (5)$$

while $\check{\mathbf{K}}$ and $\hat{\mathbf{K}}$ are undamaged stiffness operators:

$$\check{\mathbf{K}} = k_n^-(\mathbf{n} \otimes \mathbf{n}); \qquad \hat{\mathbf{K}} = k_s \mathbf{I} + (k_n^+ - k_s)(\mathbf{n} \otimes \mathbf{n}) \quad (6)$$

$\mathbf{I}$ being the identity tensor.

The expression of the damage-driving force:

$$Y_m = -\frac{\partial \psi}{\partial D} = \frac{1}{2}\left[k_n^+ \langle \llbracket u_n \rrbracket \rangle_+^2 + k_s \llbracket u_s \rrbracket^2 \right] \quad (7)$$

suggest the following definition of the equivalent opening displacement δ:

$$\delta = \left(\langle \llbracket u_n \rrbracket \rangle_+^2 + \frac{k_s}{k_n^+} \llbracket u_s \rrbracket^2 \right)^{1/2} \qquad (8)$$

whereby one obtains the damage energy release rate as:

$$Y_m = \frac{1}{2} k_n^+ \delta^2 \qquad (9)$$

and the cohesive law in the local frame attached to each point of the interface in the form:

$$t_\delta = (1-D)k_n^+ \delta \qquad (10)$$

t_δ being the equivalent scalar traction:

$$t_\delta = \left(\langle t_n \rangle_+^2 + \frac{k_n^+}{k_s} t_s^2 \right)^{1/2} \qquad (11)$$

It is worth emphasizing that the above expressions directly emanate from the potential (3); no a priori assumption is required neither on the shape of the cohesive law nor on that of the fracture locus and that mode
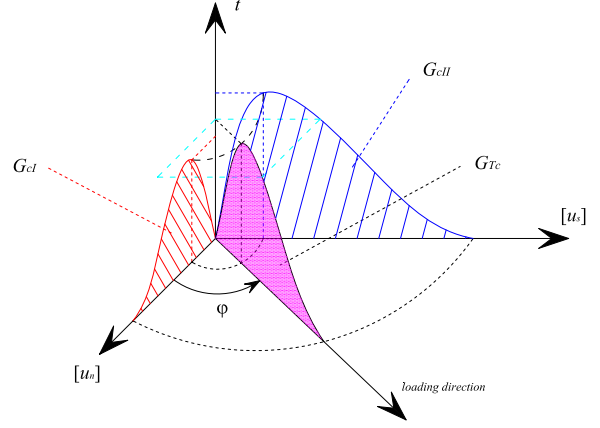
Fig. 2 Traction-relative displacement relationship and loading direction.

partition is made only based on the mode-mixity ratio defined as:

$$\beta = \sqrt{\frac{k_s}{k_n^+}} \tan \varphi \qquad (12)$$

φ being the angle that defines the loading direction:

$$\varphi = \arctan\left[\frac{\llbracket u_s \rrbracket}{\langle \llbracket u_n \rrbracket \rangle_+} \right] \in [0, +\pi/2] \qquad (13)$$

that is also used to select the appropriate traction-displacement jump relationship (Figure 2) and to compute the characteristic model parameters.

Basically, the model requires as input data the undamaged interface stiffnesses k_n^+ and k_s, that can be estimated via acoustic measurements, the pure-mode critical fracture energies G_{cI}, G_{cII}, a damage function and two interaction criteria for damage onset and decohesion propagation.

3 Element technology

A quadratic (six-noded) one-dimensional interface element is shown in figure (3). Here ξ is the local natural coordinate while x, y are the global coordinates.

Since the element undergoes large transformations, an immediate difficulty arises in the identification of the current geometry of the cohesive surface. One way to resolve this non-uniqueness is that of making reference to the mean deformed surface, that is obtained mapping the adhesive layer in the reference configuration via the mean deformation (Figure 3):

$$\bar{\chi}(\boldsymbol{X}, t) = \frac{1}{2}\left[\chi^+(\boldsymbol{X}, t) + \chi^-(\boldsymbol{X}, t) \right] \qquad (14)$$

that also permits the elimination of any ambiguity in the definition of the unit normal $\mathbf{n}$, upon which the cohesive tractions explicitly depend.

In order to obtain the director cosines of the unit tangent and normal vectors start by considering the differential

length of the line element of the mean deformed surface in the current configuration:

$$\mathrm{d}s = \sqrt{\mathrm{d}\bar{x}^2 + \mathrm{d}\bar{y}^2} \qquad (15)$$

that depend upon the isoparametric map and the updated mid-coordinates:

$$\begin{aligned}\bar{x}^j &= X^j + \tfrac{1}{2}[u_1^j + u_1^{(7-j)}] \\ \bar{y}^j &= Y^j + \tfrac{1}{2}[u_2^j + u_2^{(7-j)}]\end{aligned} \quad j = 1,\dots,nel \quad (16)$$

u^j being the nodal displacements and nel half the number of element nodes.
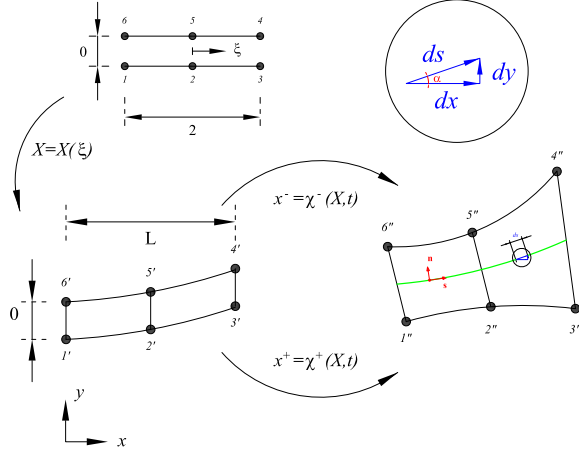
Fig. 3 Element transformations

The jacobian operator, that in the present case is a scalar, reads:

$$J = \frac{\mathrm{d}s}{\mathrm{d}\xi} = \sqrt{\left(\sum_{j=1}^{nel} N_{,\xi}^j \bar{x}^j\right)^2 + \left(\sum_{j=1}^{nel} N_{,\xi}^j \bar{y}^j\right)^2} \quad (17)$$

wereby one can compute the first derivative along the line element of any quantity A as:

$$\frac{\partial A}{\partial s} = J^{-1}\frac{\partial A}{\partial \xi} \qquad (18)$$

Accordingly, the director cosines are obtained as:

$$\begin{aligned}\mathbf{s}_x &= +\mathbf{n}_y = \cos\alpha = \frac{\mathrm{d}\bar{x}}{\mathrm{d}s} = J^{-1}\frac{\partial \bar{x}}{\partial \xi} \\ \mathbf{s}_y &= -\mathbf{n}_x = \sin\alpha = \frac{\mathrm{d}\bar{y}}{\mathrm{d}s} = J^{-1}\frac{\partial \bar{y}}{\partial \xi}\end{aligned} \qquad (19)$$

Note that relationship (18) expresses the gradient with respect to the spatial (curvilinear) coordinate of an updated Lagrangian formulation in the form:

$$\nabla_{\boldsymbol{x}}(\cdot) = \mathbf{F}^{-T}\nabla_\xi(\cdot) \qquad (20)$$

being:

$$\mathbf{F} = \nabla_\xi(\boldsymbol{x}) = \nabla_\xi(\boldsymbol{X})\,\nabla_{\boldsymbol{X}}(\boldsymbol{x}) \qquad (21)$$

the jacobian of the transformation mapping the parent element in the isoparametric space to the current (deformed) configuration.

3.1 Consistent linearization

An essential ingredient for the solution of the discretized BVP via Newton's method is the computation of the tangent stiffness tensor, that stems from the linearization:

$$\begin{aligned}\mathrm{d}_{\boldsymbol{x}}\mathbf{t}\left(\llbracket\boldsymbol{u}\rrbracket,\mathbf{n}\right) &= \mathrm{d}_{\llbracket\boldsymbol{u}\rrbracket}\mathbf{t}(\llbracket\boldsymbol{u}\rrbracket,\mathbf{n})\cdot\mathrm{d}_{\boldsymbol{x}}\llbracket\boldsymbol{u}\rrbracket \\ &\quad + \mathrm{d}_{\mathbf{n}}\mathbf{t}(\llbracket\boldsymbol{u}\rrbracket,\mathbf{n})\cdot\mathrm{d}_{\boldsymbol{x}}\mathbf{n}\end{aligned} \qquad (22)$$

The derivative of the traction vector with respect to the displacement jump defines the material tangent $\mathbf{D}_t$ whose explicit expression reads:

$$\begin{aligned}\mathbf{D}_t &= (1-D)\hat{\mathbf{K}}\,\mathrm{d}_{\llbracket\boldsymbol{u}\rrbracket}\hat{\mathbf{P}}(\llbracket\boldsymbol{u}\rrbracket) + \check{\mathbf{K}}\,\mathrm{d}_{\llbracket\boldsymbol{u}\rrbracket}\check{\mathbf{P}}(\llbracket\boldsymbol{u}\rrbracket) \\ &\quad - H_D\hat{\mathbf{K}}\hat{\mathbf{P}}(\llbracket\boldsymbol{u}\rrbracket)\otimes\,\mathrm{d}_{\llbracket\boldsymbol{u}\rrbracket}D\end{aligned} \qquad (23)$$

where H_D is a Heaviside step function, that is used to distinguish between damage loading and elastic unloading, and $\mathrm{d}_{\llbracket\boldsymbol{u}\rrbracket}D$ is the damage derivative:

$$\mathrm{d}_{\llbracket\boldsymbol{u}\rrbracket}D = \frac{\partial D}{\partial Y_m}\mathbf{I} + \frac{\partial D}{\partial Y_{mo}}\mathbf{A}(\boldsymbol{\beta}) + \frac{\partial D}{\partial G_T}\mathbf{B}(\boldsymbol{\beta}) \qquad (24)$$

that depends upon the adopted damage law, the interaction criterion for damage onset, controlled by the activation energy Y_{mo}, and the decohesion propagation condition, that takes place for a variable released energy G_T depending upon the loading direction, see also [2] for a full account.

The geometric part of the tangent consists of two contributions, namely, the derivative of the traction with respect to the normal $\mathbf{n}$ and the derivative of the unit normal $\mathbf{n}$ with respect to the spatial coordinates $\boldsymbol{x}$ [4].

The first term reads:

$$\begin{aligned}\mathrm{d}_{\mathbf{n}}\mathbf{t}(\llbracket\boldsymbol{u}\rrbracket,\mathbf{n}) &= k_n^- \left[f^-\mathbf{n}\otimes\llbracket\boldsymbol{u}\rrbracket + \langle\llbracket u_n\rrbracket\rangle_-\right] \\ &\quad + (1-D)k_n^+ \left[f^+\mathbf{n}\otimes\llbracket\boldsymbol{u}\rrbracket + \langle\llbracket u_n\rrbracket\rangle_+\right] \\ &\quad - (1-D)k_s \left[\mathbf{n}\otimes\llbracket\boldsymbol{u}\rrbracket + \mathbf{n}\cdot\llbracket\boldsymbol{u}\rrbracket\right]\end{aligned} \qquad (25)$$

with

$$f^\pm = \frac{1}{2}\left[1 \pm \mathrm{sgn}(\llbracket u_n\rrbracket)\right] \qquad (26)$$

The explicit expression of the derivative of $\mathbf{n}$, though conceptually simple, is in general quite involved since it depends on the geometry of the mean deformed surface. In the adopted implementation this has been obtained by differentiating the expressions (19) with respect to the spatial coordinates. This requires in turn the computation of second derivatives as:

$$\begin{aligned}\frac{\partial^2 A}{\partial s^2} &= \frac{\partial}{\partial s}\left(J^{-1}\frac{\partial A}{\partial \xi}\right) = J^{-1}\frac{\partial}{\partial \xi}\left(J^{-1}\frac{\partial A}{\partial \xi}\right) \\ &= J^{-2}\frac{\partial^2 A}{\partial \xi^2} - J^{-3}\frac{\partial J}{\partial \xi}\frac{\partial A}{\partial \xi}\end{aligned} \qquad (27)$$

where the natural derivative of the jacobian:

$$\frac{\partial J}{\partial \xi} = \frac{\mathrm{d}^2 s}{\mathrm{d}\xi^2} \qquad (28)$$

can be obtained from (17) by direct differentiation.

4 Numerical examples

In this section we consider the application of the model briefly discussed in the previous sections to predict the response of two adhesively-bonded assemblies. The cohesive model has been implemented within a user-defined interface element as a part of general-purpose FE code FEAP rel. 7.4 [5]. The material data sets for the adherends, made from the 5754 aluminum alloy, and the bonded interface, made from XD 4600 Ciba-Geigy epoxy adhesive, are derived from [6].

In the numerical simulation the aluminum alloy is modeled using the finite deformation logarithmic stretch-based Mises model with saturation-type isotropic hardening [7]; the elastic constants for the adherends are taken as E=70 (GPa) and $\nu = 0.33$, while the yield stresses and strain-hardening characteristics are extracted from the experimentally measured stress-strain curve as σ_y^0=100, σ_y^∞=240, H_{iso}=100 (MPa), $\beta = 20$.

The material parameters for the interface are taken as $k_n^+ = 8500$, $k_s = 750$ (N/mm³) $G_{cI} = 1.00$, $G_{cII} = 5.40$ (N/mm). The characteristic energies G_{oI}, G_{oII} have been respectively taken as a fraction of G_{cI}, G_{cII} in absence of any further information; however, for the numerical examples considered hereafter, these values have been found to have little influence on the computed response.

4.1 Shear-lap joint test

In this eample we consider a single-lap joint problem, basically consisting of two plates joined by a thin adhesive layer. The geometry of the test is shown in Figure 4 (all dimensions are in mm). The joint is loaded by prescribing diplacements at the left and right ends.
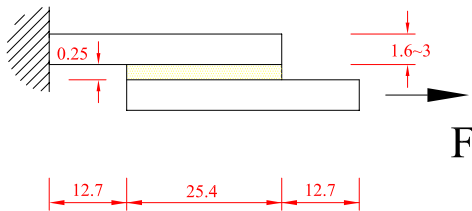
Fig. 4 Shear-lap joint. Model problem

Figures 5-6 compare, for the specimens with different adherend ticknesses, the numerically predicted load-deflection curves and the experimentally observed ones reported in [6]. As expected, plane stress elements perform better than plane strain elements for this test since the deformation in the free arms is dominated by axial tension.

The numerical simulations are recognized to capture all the major features of the macroscopic response of the structure, that include a geometric hardening effect due to the joint rotation, that produces the re-alignment of the joint arms, and a stress state in the adhesive layer that becomes progressively shear-dominated as the cohesive zone develops.
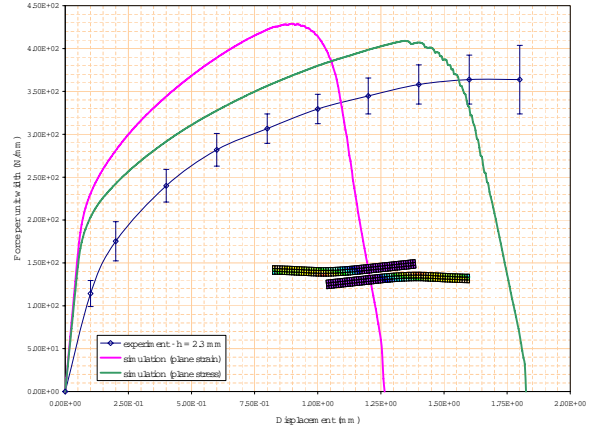
Fig. 5 Shear-lap joint. Numerical vs experimental results. Adherend thickness 2.0/3.0 mm
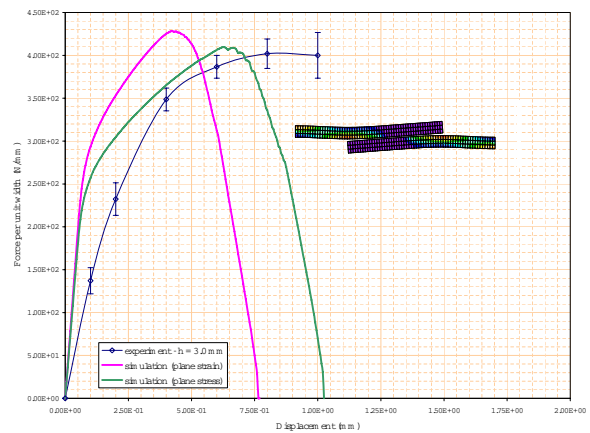
Fig. 6 Shear-lap joint. Numerical vs experimental results. Adherend thickness 3.0/3.0 mm

4.2 T-peel test

This example refers to the T-peel test, often used to evaluate the peel strength of adhesives. The geometry of the sample is shown in Figure 7 (all dimensions are in mm). Load is simulated via displacement control at the ends of vertical arms.
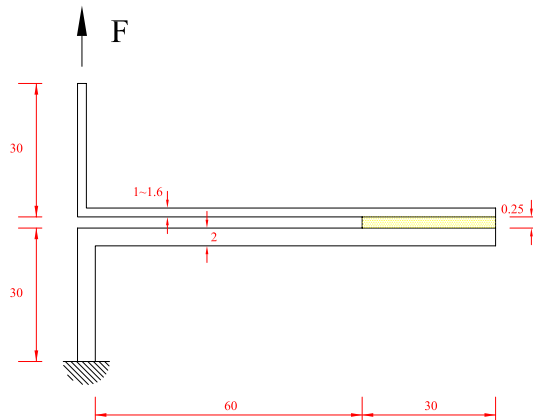
Fig. 7 T-peel joint. Model problem
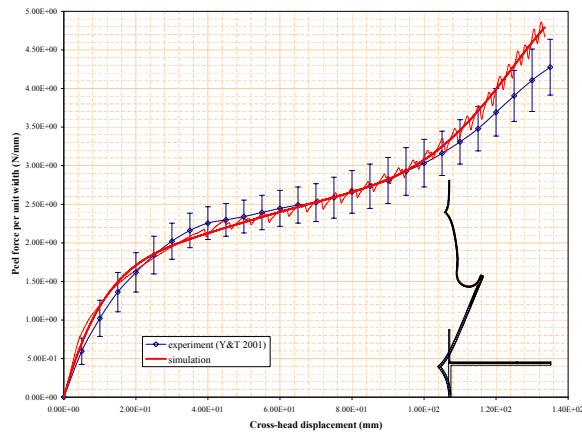
Fig. 8 T-peel joint. Numerical vs experimental results. Adherend thickness 1.0/2.0 mm
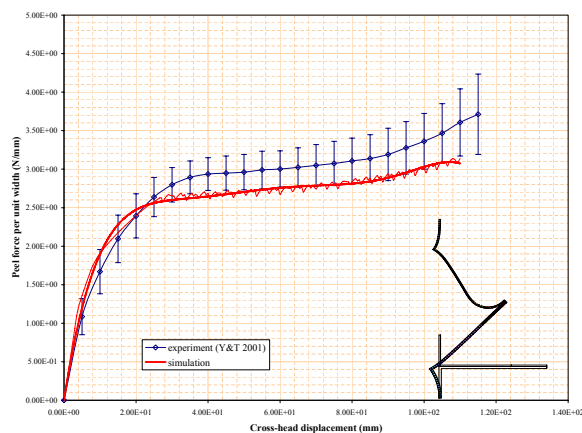
Fig. 9 T-peel joint. Numerical vs experimental results. Adherend thickness 1.3/2.0 mm
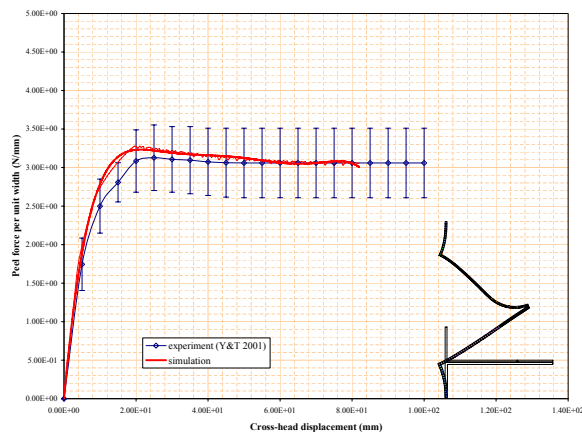
Fig. 10 T-peel joint. Numerical vs experimental results. Adherend thickness 1.6/2.0 mm

Plane strain elements are used for this test since the deformation of the adherends is dominated by bending. Three different adherend thickness combinations are considered (1.0/2.0, 1.3/2.0 and 1.6/2.0 mm) and the relevant numerically predicted load-deflection curves

are compared in Figures 8-10 with those experimentally observed and documented in [6].

Unlike the previous example, in this geometry the response of the interface is essentially mode-I dominated; however, the numerical simulations show that adhesive fracture is accompanied by extensive plastic deformation both in the vicinity of the active process zone and in the region of the right-angle bend, which does not allow the measured force to be taken as a measure of the interfacial strength under peeling.

All the salient features of the macroscopic response of the structure, that exhibits a marked sensitivity of the peel force to the adherend thickness, large rotations and bending asymmetry are well captured by the simulation, as it can also be appreciated from the deformed shape of the samples that are also reported in the same Figures 8-10.

Acknowledgements

5 References

[1] R. de Borst. Numerical aspects of cohesive-zone models. *Engineering Fracture Mechanics*, 70:1743–1757, 2003.

[2] N. Valoroso and L. Champaney. A damage-mechanics-based approach for modelling decohesion in adhesively bonded assemblies. *Engineering Fracture Mechanics*, 73:2774–2801, 2006.

[3] O. Allix and A. Corigliano. Geometrical and interfacial non-linearities in the analysis of delamination in composites. *International Journal of Solids and Structures*, 36:2189–2216, 1999.

[4] M. Ortiz and A. Pandolfi. Finite-deformation irreversible cohesive elements for three-dimensional crack-propagation analysis. *International Journal for Numerical Methods in Engineering*, 44:1267–1282, 1999.

[5] R. L. Taylor. *FEAP - User Manual*. University of California at Berkekey, Berkeley, USA, 2002.

[6] Q. D. Yang and M. Thouless. Mixed-mode fracture analyses of plastically-deforming adhesive joints. *International Journal of Fracture*, 110:175–187, 2001.

[7] J. C. Simo. Algorithms for static and dynamic multiplicative plasticity that preserve the classical return mapping schemes of the infinitesimal theory. *Computer Methods in Applied Mechanics and Engineering*, 99:61–112, 1992.